ARMY RESEARCH LABORATORY

Analysis of the Ferroelectric Thin Films Deposited By Pulsed Laser Deposition On Oxide and Fluoride Substrates

S. Sengupta, W.E. Kosik, J.D. Demaree, and L.C. Sengupta

ARL-TR-655

December 1994

The findings in this report are not to be construed as an official Department of the Army position unless so designated by other authorized documents.

Citation of manufacturer's or trade names does not constitute an official endorsement or approval of the use thereof.

Destroy this report when it is no longer needed. Do not return it to the originator.

REPORT DOCUMENTATION PAGE

Form Approved
OMB No. 0704-0188

1. AGENCY USE ONLY *(Leave blank)*	2. REPORT DATE	3. REPORT TYPE AND DATES COVERED
	December 1994	

4. TITLE AND SUBTITLE
Analysis of the Ferroelectric Thin Films Deposited by Pulsed Laser Deposition on Oxide and Fluoride Substrates

5. FUNDING NUMBERS

6. AUTHOR(S)
S. Sengupta, W.E. Kosik, J.D. Demaree, and L.C. Sengupta

7. PERFORMING ORGANIZATION NAME(S) AND ADDRESS(ES)
Army Research Laboratory
Watertown, MA 02172-0001
AMSRL-MA-CA

8. PERFORMING ORGANIZATION REPORT NUMBER
ARL-TR-655

9. SPONSORING/MONITORING AGENCY NAME(S) AND ADDRESS(ES)

10. SPONSORING/MONITORING AGENCY REPORT NUMBER

11. SUPPLEMENTARY NOTES

12a. DISTRIBUTION/AVAILABILITY STATEMENT
Approved for public release; distribution unlimited.

12b. DISTRIBUTION CODE

13. ABSTRACT

This work has been carried out as part of an ongoing investigation in which thin film ferroelectric phase shifters are being constructed, tested, and optimized. These phase shifters will be incorporated into multi-element phased array antennas where the beam steering material used was $Ba_{0.6}Sr_{0.4}TiO_3$ (BSTO) and BSTO with 1 wt.% oxide additive. Thin films of BSTO have been deposited by pulsed laser deposition (PLD) onto various oxide and fluoride substrates. These include oxide substrates such as magnesium oxide (MgO), sapphire (Al_2O_3), lanthanum aluminate ($LaAlO_3$), neodymium gallate ($NdGaO_3$) , and fluoride substrates such as rubidium manganese fluoride ($RbMnF_3$). These substrates were selected for their relatively low dielectric constants and good lattice matches to the ferroelectric thin film compound (a =3.94 Å). The substrate / film interfaces, areal film thicknesses and compositional variations have been studied using Rutherford Backscattering Spectroscopy (RBS), and physical thicknesses have been measured using a profilometer. The orientation of the thin films was investigated using glancing angle x-ray diffraction. Various electrodes have been used in order to optimize the electronic properties of the films. These electronic properties were tested at 30 KHz using an HP 4194A impedance analyzer . The measured electronic properties include the dielectric constant, and the tunability (change in the dielectric constant with applied electric field). The electronic properties have been correlated to the results derived from RBS and x-ray data and will be discussed.

14. SUBJECT TERMS
Ferroelectric, BSTO, PLD, Oxide Substrates, Fluoride Substrates

15. NUMBER OF PAGES
13

16. PRICE CODE

17. SECURITY CLASSIFICATION OF REPORT	18. SECURITY CLASSIFICATION OF THIS PAGE	19. SECURITY CLASSIFICATION OF ABSTRACT	20. LIMITATION OF ABSTRACT
Unclassified	Unclassified	Unclassified	UL

Contents

Figures

Tables

INTRODUCTION

Phased array antennas can steer transmitted or received signals either linearly or in two dimensions without mechanically oscillating the antenna. These antennas are currently constructed using ferrite phase shifting elements. Due to the circuit requirements necessary to operate these antennas, they are costly, large and heavy. Therefore, the use of these antennas has been limited primarily to military applications which are strategically dependent on such capabilities. In order to make these devices available for many other commercial and military uses, the basic concept of the antenna must be improved. If ferroelectric materials could be used for the phase shifting element instead of ferrites, phased array antennas could be significantly improved.

A ceramic Barium Strontium Titanate, $Ba_{1-x}Sr_xTiO_3$, (BSTO), phase shifter using a planar microstrip construction has been demonstrated[1]. In order to meet the required performance specifications (e.g.,maximum phase shifting ability), the electronic properties in the low frequency (KHz) and microwave regions (GHz) must be optimized. As part of this optimization process, various composites of BSTO and non-ferroelectric oxides have been formulated.

In order to obtain higher operating frequencies and to decrease the voltage requirements, thin film fabrication of the above candidate materials is necessary. This paper outlines preliminary work on the PLD of undoped and modified BSTO on various substrates. The composition at the substrate/film interface and the bulk of the film have been obtained using RBS. Glancing angle x-ray diffraction has been used to determine the orientation of the films. Various electroding combinations were used in order to optimize the electronic properties of the films and these properties were measured for some of the films using an HP 4194A impedance analyzer. The results of these measurements will be discussed and correlated to the RBS and x-ray diffraction data.

EXPERIMENTAL

The PLD was accomplished using a krypton-fluoride excimer laser with a wavelength of 248 nm and a repetition rate of 10 Hz. The average pulse energy was 300 mJ with a 20 ns pulse width. The oxygen partial pressure in the chamber was 150 mT and the substrate temperature was 520 ^{0}C, which was monitored by a thermocouple clamped between the heater and the substrate. The substrate was parallel to target and their separation distance was maintained at 48 mm. The powder pressed ceramic targets were prepared according to a description published previously [2].

The lattice parameters and dielectric constants of the substrates used in this experiment are listed in Table 1. Prior to PLD, the substrates underwent a cleaning cycle which included an ultrasonic cycle of TCE followed by two methanol ultrasonic cycles. The samples were then rinsed with methanol and air dried.

TABLE 1. Relevant Physical Parameters of the Single Crystals Used as Substrates

	SUBSTRATE				
	MgO	Al_2O_3	$LaAlO_3$	$NdGaO_3$	$RbMnF_3$
Lattice parameter (Å)	4.21	4.76	3.79	3.84	4.24
Dielectric constant (300K)	10	11	23	20	15

The targets chosen for this report were $Ba_{0.6}Sr_{0.4}TiO_3$ (BSTO), BSTO with 1 wt% alumina and BSTO with 1 wt% of an additive oxide, referred to hereafter as oxide III. A Dektak-200 profilometer was used to measure the films thickness which was approximately 5000 Å on all the substrates.

In order to measure the electronic properties of the films, two different ground plane electrodes were used. For the first system, the Ti/Pt electrode was sputtered sequentially with Xe ions from a Zymet Z-100 ion implantation unit. A target angle of 30^0 with respect to the incident beam was used. The thickness of the sputtered Ti layer was 1000 Å and the thickness of the overlying Pt layer was 1500 Å. For the second system, Ruthenium oxide (RuO_2) was sputtered onto the substrates at a substrate temperature of 200^0C and a O_2/Ar ratio of 1:4 with a total pressure of 10 mT. The Ruthenium oxide films were 3000 Å thick. The resistivity of the as-deposited films were in the order of 160 μohms-cm. They were annealed at 600^0C for 30 minutes to lower the resistivity and were cooled by furnace quenching. The resistivity of the annealed films were measured to be 110 μohms-cm. The thicknesses of the top electrodes were measured to be approximately 3000 Å using a Dektak-200 profilometer. The metallized films used for the electrical measurements were: (1) Sapphire/Ti/Pt/BSTO with 1 wt% alumina / Au, (2) Sapphire/RuO_2/BSTO/Au and (3) Sapphire/RuO_2/BSTO with 1 wt% oxide III/Au. The BSTO thickness of (1) was measured to be 8000 Å while the thickness of combinations (2) and (3) was measured to be about 6000 Å.

The RBS technique used involve the acceleration of He^+ ions to 2 MeV by a National Electrostatics Corporation (NEC) tandem pelletron accelerator. This He^+ ion beam is collimated to a 1 mm diameter beam which is incident upon the film/crystal substrate. The scattered helium ions were detected at a backscattering angle of 170^0 with a surface barrier detector with a system energy resolution of 20 to 25 KeV. The energy detection system is calibrated with a standard prior to data acquisition. The elements in the crystal are determined from the detected energies of the backscattered ions which are related to the mass of the atoms. The composition of the films/crystals were obtained by utilizing the software program RUMP to fit the data [3].

The glancing angle x-ray measurements were performed using a Rigaku RU 200 rotating anode x-ray diffractometer. The entrance slit had a width of 0.2^0 and the angle of incidence of the Cu Kα (λ=1.5415 Å) beam was set at 1^0. The sample interval was 0.02^0 and the scan rate was 9^0/minute.

The dielectric constant (ε') and % tunability were determined for all thin film/substrate combination. The % tunability of a material is determined using the following equation:

$$\% \text{ tunability} = \{ \varepsilon'(0) - \varepsilon'(Vapp)\}/ \{\varepsilon'(0)\} \quad (1)$$

The tunability measurements were taken with an applied electric field which ranged from 0 to +/- 8.0 V/micron (μm). The electronic properties were measured at a frequency of 30 KHz. Capacitance versus voltage (C-V) measurements for the films were taken using an HP4194 impedance / phase gain analyzer. The voltage was applied internally through the HP 4194A and was varied from -8.0 V to +8.0 V.

RESULTS AND DISCUSSION

Glancing Angle X-ray Results

Bare Substrates

The glancing angle x-ray diffraction pattern (GAXRD) for the BSTO / 1wt% oxide III film deposited on $RbMnF_3$ is shown in Figure 1. As shown in the figure, all of the x-ray peaks match the peaks of the of the target material, which is shown in the inset. However, there is evidence of the presence of a small amount of a secondary Ba-rich ($Ba_{1.91}Sr_{0.09}TiO_4$) phase. The preferred (110) orientation of the film is indicated by the higher relative intensity of the (110) peak as shown in the x-ray pattern.

Fig. 2 shows the GAXRD of BSTO/1 wt.% oxide III deposited on $NdGaO_3$. The pattern does not show a good match with the target material and is indicative of an amorphous film. We observed the same type of amorphous film quality for the BSTO/oxide III deposited on $LaAlO_3$.

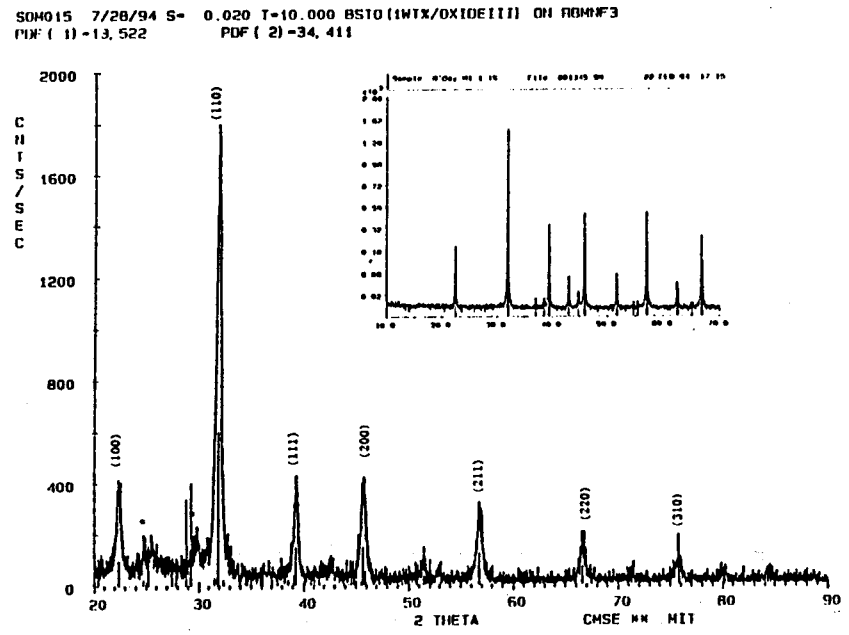

Figure 1. Glancing Angle X-ray Diffraction Pattern of BSTO/1wt% oxide III Film Deposited on $RbMnF_3$. Inset shows x-ray pattern of the target material.

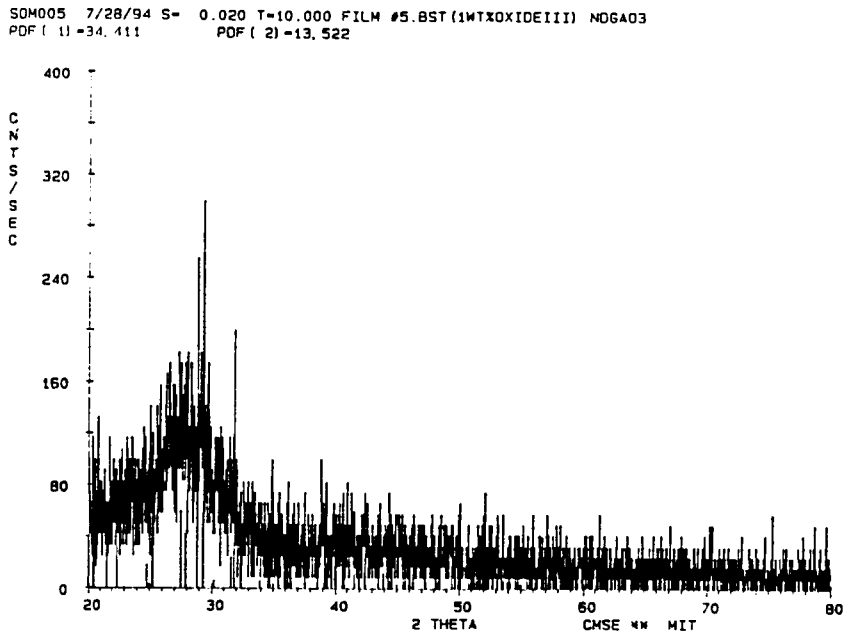

Figure 2. Glancing Angle X-ray Diffraction Pattern of BSTO/1wt% Oxide III Film Deposited on $NdGaO_3$.

Metallized Films

Fig. 3 shows the GAXRD pattern for the BSTO (with 1 wt% alumina) film deposited on the platinized sapphire substrate. The inset shows the powder diffraction pattern of the target material. It was observed from the x-ray pattern of the target that a secondary phase ($Ba_3Al_{10}TiO_{20}$; marked "*") is present. As shown in the figure the dominant peak for the pattern is the (220) peak. We measured a slight systematic shift in the position of the peaks which may be attributed to the change in the lattice parameter of the material due to the dopant.

In Fig.4, the GAXRD pattern of the BSTO (with 1 wt.% oxide III) film deposited on the RuO_2/sapphire substrate is shown. The inset is the x-ray pattern of the BSTO target material. The pattern does not indicate the presence of any secondary phase. The peaks located at 28.1^0 and 54.2^0 2θ positions are those of RuO_2.

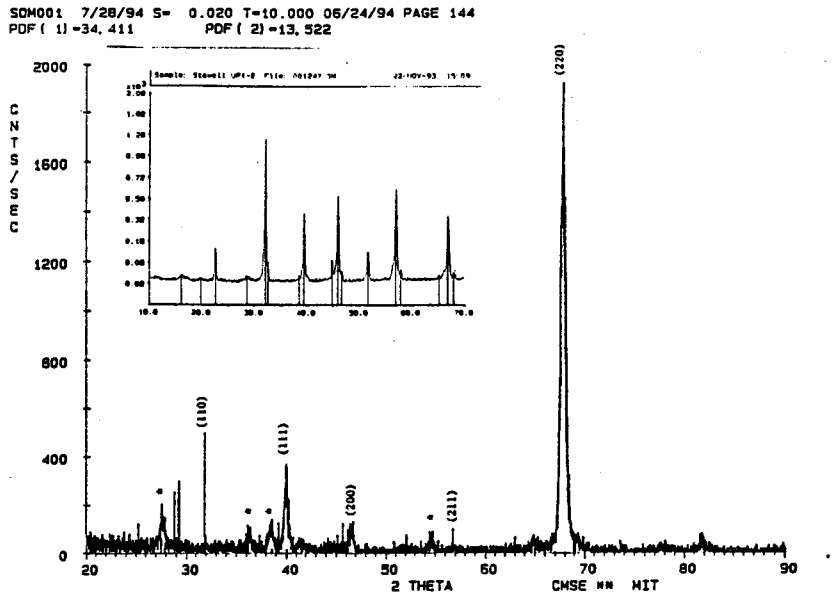

Figure 3. Glancing Angle X-ray Diffraction Pattern for the BSTO (with 1 wt% alumina) Film Deposited on the Platinized Sapphire Substrate ("*" indicates $Ba_3Al_{10}TiO_{20}$ phase). The inset shows the powder diffraction pattern of the target material.

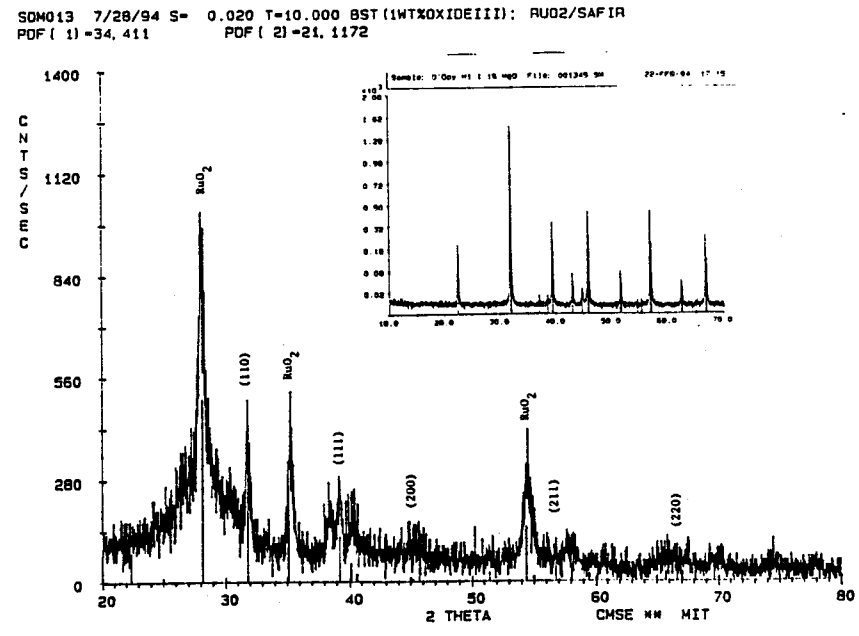

Figure 4. Glancing Angle X-ray Diffraction Pattern of the BSTO (with 1 wt% oxide III) Film Deposited on the RuO_2/Sapphire Substrate. The inset is the x-ray pattern of the ceramic target.

SEM/EDS Results

The presence of a secondary phase in the films evident from the x-ray patterns discussed above were confirmed by SEM/EDS results. Another Ba-rich phase in the BSTO/oxide III film deposited on $RbMnF_3$ is evident from the light areas in the SEM micrograph shown in Fig. 5. The "x" mark shows the location of this Ba-rich phase confirmed by EDS. Fig. 6 contains the SEM micrograph of the BSTO/Alumina thin film deposited on platinized sapphire. The presence of a secondary phase in the material is revealed in the micrograph by the small light regions. EDS performed on these areas also indicated the presence of a Ba-rich phase as well as the presence of a segregated strontium deficient titanate phase. This type of segregation was also observed in the bulk ceramic used as the ablation target.

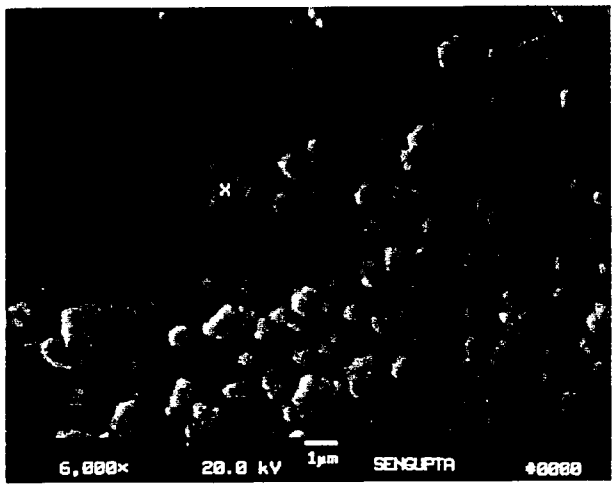

Figure 5. SEM Micrograph of BSTO/1 wt% Oxide III Film Deposited on $RbMnF_3$.

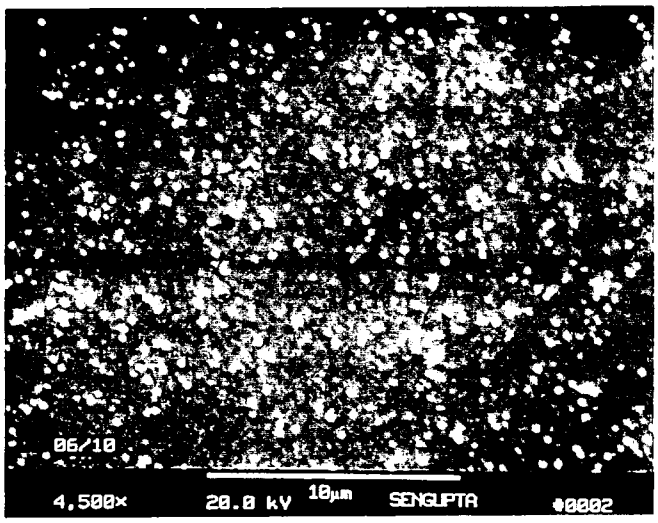

Figure 6. SEM Micrograph of BSTO/1 wt% Alumina Film Deposited on Platinized Sapphire.

RBS Results

Fig. 7, shows the RBS spectrum of BSTO/1 wt% oxide III film deposited on $NdGaO_3$. The dotted line is the experimental data, while the solid line represents the theoretical fit to the data using RUMP simulation code. The data was fit by substracting the RBS spectrum of the substrate from the spectrum of the BSTO/1 wt% oxide III film deposited on the substrate and by assuming a composition of $Ba_{0.6}Sr_{0.4}TiO_3$ (1wt% oxide III) for the film. The goodness of the fit indicates that the film has a composition close to that of the ceramic target which was $Ba_{0.6}Sr_{0.4}TiO_3$ (1wt.% oxide III). However, GAXRD shown in Fig. 2 reveals that the film is noncrystalline.

The RBS spectra of the BSTO films deposited on the other substrates also show close agreement of the thin film elemental composition with that of the original ceramic target.

Electronic Measurements

Fig. 8, shows the capacitance versus voltage characteristics for the BSTO (undoped) film deposited on RuO_2/MgO. The curve shows a symmetric capacitance-voltage relationship which is characteristic of paraelectric films. The dielectric constant at zero bias was calculated to be 1474 and the tunability is 88 % at a field of 7.5 V/μm. The bulk undoped material has a dielectric constant of 3300 and a tunability of 20 % at 0.73 V/μm. It has been previously shown that the dielectric constant in ferroelectric films are inherently less than the bulk ceramics due to oxygen defects at the electrode/ film interface [4]. Also any porosity and/or leakage current in the films will tend to decrease the dielectric constants obtained.

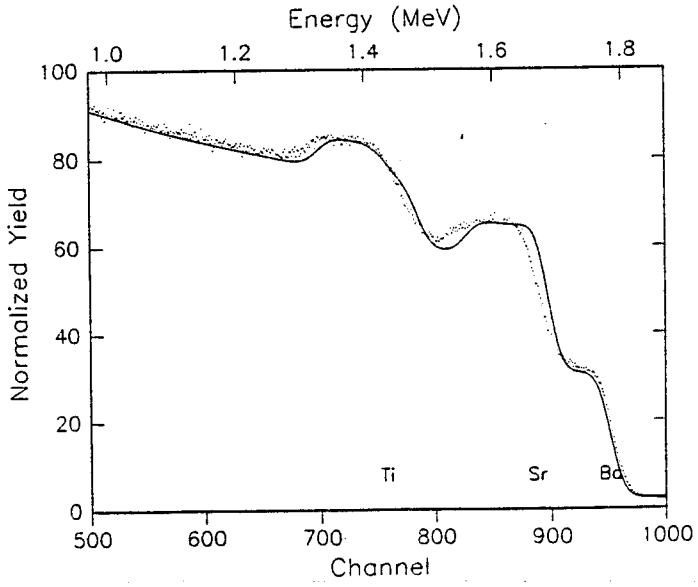

Figure 7. RBS Spectrum of BSTO/1 wt% Oxide III Film Deposited on $NdGaO_3$, [Experimental data (dotted line) and RUMP fit (solid line)].

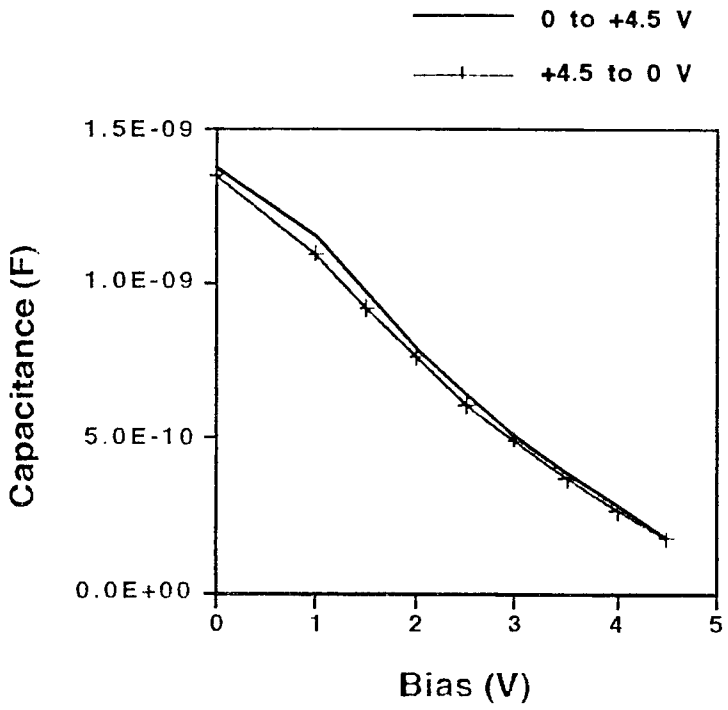

Figure 8. Capacitance versus Voltage for BSTO (undoped) Deposited on RuO_2/MgO with Pt Top Electrode.

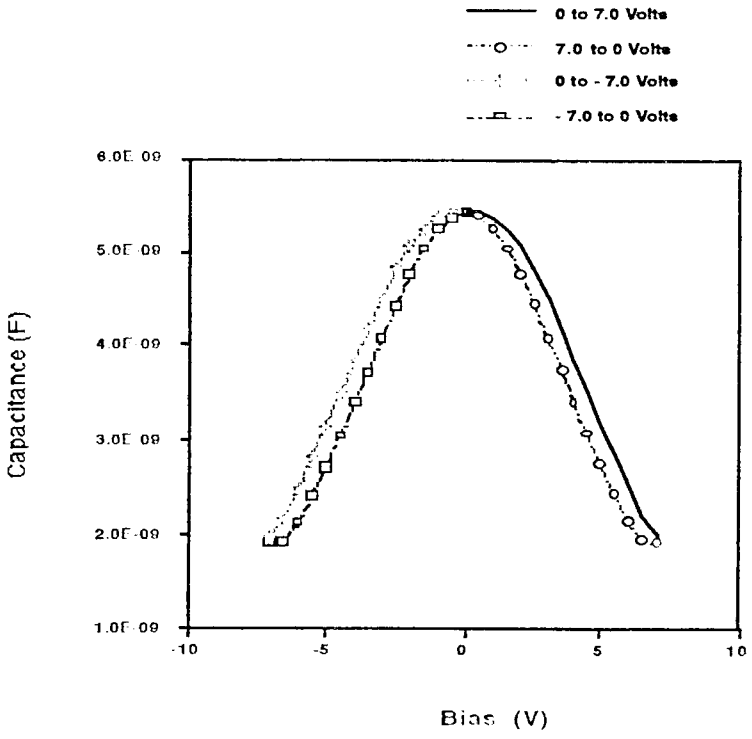

Figure 9. Capacitance versus Voltage for BSTO/1 wt% Alumina Deposited on Platinized Sapphire with Au Top Electrode.

The C-V curve for the BSTO/1 wt% alumina film deposited on platinized sapphire is shown in Fig. 9. The curve shows a typical paraelectric behavior, (i.e. a symmetric capacitance), with positive and negative bias applied. The dielectric constant at zero voltage calculated from this curve is 189. The tunability obtained up to 6.3 V/μm was 40%. The value for the dielectric constant found in the bulk ceramic target of BSTO/1 wt% alumina was 2607 and a tunability of 46% at 2.7 V/μm. The low value for the dielectric constant in the film relative to that in the bulk ceramic target may be attributed to the porosity of the film , the presence of leakage current (on the order of 10^{-5} A) and also to the segregation of the secondary phase as was shown in Fig. 6.

The capacitance versus voltage for the BSTO/1 wt% oxide III film deposited on RuO_2/sapphire is shown in Fig. 10. This curve also shows the typical paraelectric behavior of symmetric capacitance versus voltage behavior. The value for the zero voltage dielectric constant is 398 and the tunability is 79% at 2.0 V/μm. The bulk ceramic dielectric constant was 1276 and the tunability was 16% with 2.3V/μm. The decreased value of the dielectric constant in the film is again attributed to the porosity of the film and the leakage current observed in the film.

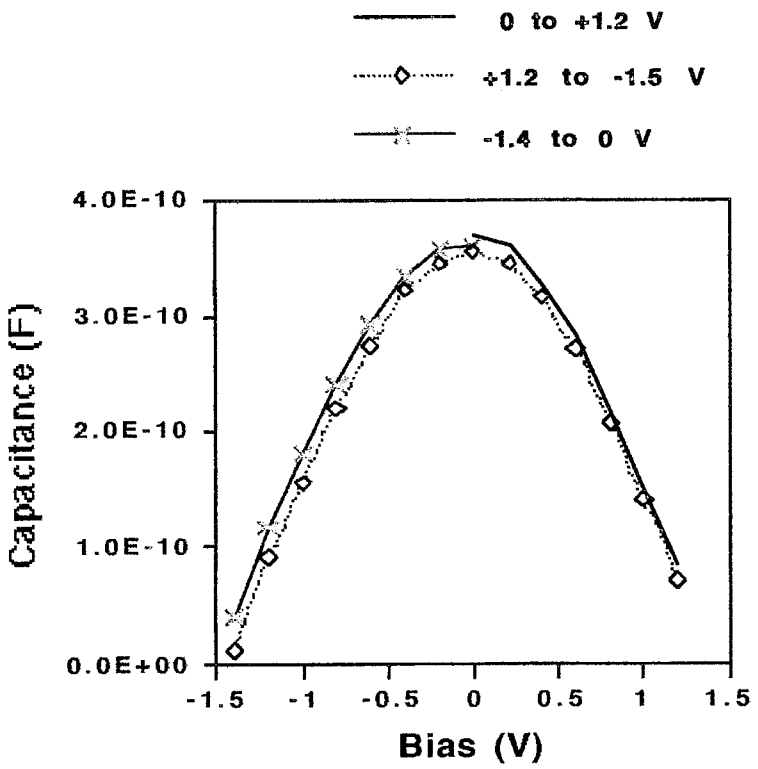

Figure 10. Capacitance versus Voltage for BSTO/1 wt.% Oxide III Deposited on RuO_2/ Sapphire with Au Top Electrode.

CONCLUSION

Thin films of both undoped and oxide modified BSTO have been deposited by PLD onto oxide and fluoride substrates. It was shown that in case of $RbMnF_3$ the film was preferentially oriented and contained a secondary phase. The film deposited on $NdGaO_3$ was amorphous; however, RBS confirmed a good agreement of film composition relative to the target materials. The BSTO/1wt.% alumina film deposited on the platinized substrate showed similar phase segregation as the ceramic material. The oxide modified film deposited on RuO_2/sapphire substrate did not show any evidence of a secondary phase. The electronic properties of the undoped and oxide modified BSTO thin films exhibited similar behavior relative to the bulk material. The dielectric constant and the tunability of the undoped BSTO film are higher than that of the doped films.

We have shown that the tailoring of the electronic properties of BSTO thin films is possible through the incorporation of metal oxides. Further investigation of such tailoring through the incorporation of other oxides is underway.

ACKNOWLEDGMENTS

The authors would like to thank A. Kirkpatrick of Epion Corp., Bedford, MA, N. Sonnenburg of CPRL, M.I.T., A. Cassanho, CMSE, M.I.T., R. Sahagian of Implant Sciences, Wakefield, MA and P.Wong of ARL, for their help.

REFERENCES

[1] R.W. Babbitt, T. E. Koscica, and W.E. Drach, "Planar Microwave Electro-optic Phase Shifters," *Microwave Journal* , vol. 35, pp. 63-79, June 1992.

[2] L.C. Sengupta, S. Stowell, E. Ngo, M.E. O'Day and R. Lancto, *J. of Integrated Ferroelectrics*, in press, (1994).

[3] L.R. Doolittle, *Nuclear Instru. Meth.*, vol B9, p. 334 (1985).

[4] C.J. Brennan, *Integrated Ferroelectrics*, vol. 2, pp.73-82 (1992).

DISTRIBUTION LIST

No. of Copies	To
1	Office of the Under Secretary of Defense for Research and Engineering, The Pentagon, Washington, DC 20301
	Director, U.S. Army Research Laboratory, 2800 Powder Mill Road, Adelphi, MD 20783-1197
1	ATTN: AMSRL-OP-SD-TP, Technical Publishing Branch
1	AMSRL-OP-SD-TA, Records Management Administrator
	Director, U.S. Army Research Laboratory, 2800 Powder Mill Road, Adelphi, MD 20783-1197
1	ATTN: Technical Library
	Commander, Defense Technical Information Center, Cameron Station, Building 5, 5010 Duke Street, Alexandria, VA 23304-6145
2	ATTN: DTIC-FDAC
1	MIA/CINDAS, Purdue University, 2595 Yeager Road, West Lafayette, IN 47905
	Commander, Army Research Office, P.O. Box 12211, Research Triangle Park, NC 27709-2211
1	ATTN: Information Processing Office
	Commander, U.S. Army Materiel Command, 5001 Eisenhower Avenue, Alexandria, VA 22333
1	ATTN: AMCSCI
	Commander, U.S. Army Materiel Systems Analysis Activity, Aberdeen Proving Ground, MD 21005
1	ATTN: AMXSY-MP, H. Cohen
	Commander, U.S. Army Missile Command, Redstone Arsenal, AL 35809
1	ATTN: AMSMI-RD-CS-R/Doc
	Commander, U.S. Army Armament, Munitions and Chemical Command, Dover, NJ 07801
2	ATTN: Technical Library
	Commander, U.S. Army Natick Research, Development and Engineering Center, Natick, MA 01760-5010
1	ATTN: DFAS-IN-EM-TL, Technical Library
	Commander, U.S. Army Satellite Communications Agency, Fort Monmouth, NJ 07703
1	ATTN: Technical Document Center
	Commander, U.S. Army Tank-Automotive Command, Warren, MI 48397-5000
1	ATTN: AMSTA-ZSK
1	AMSTA-TSL, Technical Library
	Commander, White Sands Missile Range, NM 88002
1	ATTN: STEWS-WS-VT
	President, Airborne, Electronics and Special Warfare Board, Fort Bragg, NC 28307
1	ATTN: Library

No. of Copies	To
	Director, U.S. Army Research Laboratory, Weapons Technology, Aberdeen Proving Ground, MD 21005-5066
1	ATTN: AMSRL-WT
	Commander, Dugway Proving Ground, UT 84022
1	ATTN: Technical Library, Technical Information Division
	Commander, U.S. Army Research Laboratory, 2800 Powder Mill Road, Adelphi, MD 20783
1	ATTN: AMSRL-SS
	Director, Benet Weapons Laboratory, LCWSL, USA AMCCOM, Watervliet, NY 12189
1	ATTN: AMSMC-LCB-TL
1	AMSMC-LCB-R
1	AMSMC-LCB-RM
1	AMSMC-LCB-RP
	Commander, U.S. Army Foreign Science and Technology Center, 220 7th Street, N.E., Charlottesville, VA 22901-5396
3	ATTN: AIFRTC, Applied Technologies Branch, Gerald Schlesinger
	Commander, U.S. Army Aeromedical Research Unit, P.O. Box 577, Fort Rucker, AL 36360
1	ATTN: Technical Library
	U.S. Army Aviation Training Library, Fort Rucker, AL 36360
1	ATTN: Building 5906-5907
	Commander, U.S. Army Agency for Aviation Safety, Fort Rucker, AL 36362
1	ATTN: Technical Library
	Commander, Clarke Engineer School Library, 3202 Nebraska Ave., N, Fort Leonard Wood, MO 65473-5000
1	ATTN: Library
	Commander, U.S. Army Engineer Waterways Experiment Station, P.O. Box 631, Vicksburg, MS 39180
1	ATTN: Research Center Library
	Commandant, U.S. Army Quartermaster School, Fort Lee, VA 23801
1	ATTN: Quartermaster School Library
	Naval Research Laboratory, Washington, DC 20375
2	ATTN: Dr. G. R. Yoder - Code 6384
	Chief of Naval Research, Arlington, VA 22217
1	ATTN: Code 471
	Commander, U.S. Air Force Wright Research & Development Center, Wright-Patterson Air Force Base, OH 45433-6523
1	ATTN: WRDC/MLLP, M. Forney, Jr.
1	WRDC/MLBC, Mr. Stanley Schulman

No. of Copies	To
	U.S. Department of Commerce, National Institute of Standards and Technology, Gaithersburg, MD 20899
1	ATTN: Stephen M. Hsu, Chief, Ceramics Division, Institute for Materials Science and Engineering
1	Committee on Marine Structures, Marine Board, National Research Council, 2101 Constitution Avenue, N.W., Washington, DC 20418
1	Materials Sciences Corporation, Suite 250, 500 Office Center Drive, Fort Washington, PA 19034
1	Charles Stark Draper Laboratory, 555 Technology Square, Cambridge, MA 02139
	Wyman-Gordon Company, P.O. Box 8001, North Grafton, MA 01536-8001
1	ATTN: Technical Library
	General Dynamics, Convair Aerospace Division, P.O. Box 748, Fort Worth, TX 76101
1	ATTN: Mfg. Engineering Technical Library
	Plastics Technical Evaluation Center, PLASTEC, ARDEC, Bldg. 355N, Picatinny Arsenal, NJ 07806-5000
1	ATTN: Harry Pebly
1	Department of the Army, Aerostructures Directorate, MS-266, U.S. Army Aviation R&T Activity - AVSCOM, Langley Research Center, Hampton, VA 23665-5225
1	NASA - Langley Research Center, Hampton, VA 23665-5225
	U.S. Army Vehicle Propulsion Directorate, NASA Lewis Research Center, 2100 Brookpark Road, Cleveland, OH 44135-3191
1	ATTN: AMSRL-VP
	Director, Defense Intelligence Agency, Washington, DC 20340-6053
1	ATTN: ODT-5A (Mr. Frank Jaeger)
	U.S. Army Communications and Electronics Command, Fort Monmouth, NJ 07703
1	ATTN: Technical Library
	U.S. Army Communications and Electronics Command, Intelligence and Electronic Warfare Center, Fort Monmouth, NJ 07703-5211
1	ATTN: Frank Elmer, AMSEL-RD-IEW-TAE-M
	U.S. Army Research Laboratory, Electronic Power Sources Directorate, Fort Monmouth, NJ 07703
1	ATTN: AMSRL-EP-M, W. C. Drach
1	AMSRL-EP-M, T. E. Koscica
1	AMSRL-EP-M, R. W. Babbit
	Director, U.S. Army Research Laboratory, Watertown, MA 02172-0001
2	ATTN: AMSRL-OP-WT-IS, Technical Library
20	Authors